

NOTICE WARNING CONCERNING COPYRIGHT RESTRICTIONS:
The copyright law of the United States (title 17, U.S. Code) governs the making of photocopies or other reproductions of copyrighted material. Any copying of this document without permission of its author may be prohibited by law.

**Optimization of Mechanisms
for Force Generation
by Using Pulleys and Spring**

Tokuji Okada

CMU-RI-TR-85-14 (3)

The Robotics Institute
Carnegie-Mellon University
Pittsburgh, Pennsylvania 15213

September 1985

Copyright © 1985 Carnegie-Mellon University

Permanent address: Electrotechnical Laboratory, 1-1-4 Umezono Sakura-mura, Niihari-gun, Ibaraki, Japan. This research was done while the author was visiting the Robotics Institute, Carnegie-Mellon University.

629.892

C28Y

85-14

Rep.3

Table of Contents

| | |
|--|----|
| 1. Introduction | 2 |
| 2. Description of Mechanism for Force Generation | 2 |
| 3. Force Generation by Using Pulleys and Spring | 4 |
| 3.1. Link Mechanism | 4 |
| 3.2. Analyses of Motion and Force Members of the Mechanism | 5 |
| 3.3. Relationship Between Force and Deformation of the Mechanism | 8 |
| 4. Optimization of Force Generation Mechanism | 9 |
| 4.1. Analytical Method | 9 |
| 4.2. Approximate Method | 11 |
| 5. Design of Pulleys and Experimental Results | 16 |
| 5.1. Circular Pulley | 16 |
| 5.2. Fusee | 16 |
| 5.3. Flat Pulleys of Non-Circular-Shape | 17 |
| 5.4. Experimental Results | 17 |
| 6. Conclusion | 18 |

List of Figures

| | |
|--|----|
| Figure 1: Basic mechanism for obtaining the stretch force | 24 |
| Figure 2: Various kinds of mechanisms for generating the force | 24 |
| Figure 3: Calculated results of the relation between H and F under such conditions that $h = r_0 = 100\text{mm}$, $k = 0.1\text{Kg/mm}$ and $30^\circ \leq \theta \leq 100^\circ$. The value of a in (b), (c), (d), (e) and (f) are $3/5r_0$, $2/5r_0$, $3/4r_0$, $1/6r_0$ and $2/3r_0$, respectively. Parameters b and c are $1/3r_0$ and $3/4r_0$, respectively. | 25 |
| Figure 4: Proposed mechanism for the force generation | 25 |
| Figure 5: Geometrical illustration for analyzing equilibrium of the mechanism in force | 26 |
| Figure 6: Calculated relation between H and F when circular pulleys are used in the complex mechanism under such conditions that $h = 95\text{mm}$, $r_0 = 35\text{mm}$, $r_1 = 7.5\text{mm}$, $r_2 = 5\text{mm}$, $L_0 = 19.05\text{mm}$, $k = 0.14\text{Kg/mm}$, $Q = 0.5\text{Kg}$ and $40^\circ \leq \theta \leq 100^\circ$. The curve c_0 is obtained under $r_3 = 0$. The curves c_1 to c_4 increase r_3 with the increment 2mm in this order. | 26 |
| Figure 7: Calculated relation between H and F when circular pulleys are used in the simple mechanism under the same conditions to those used in the complex mechanism. The curve c_0 is obtained under $r_3 = 0$. The curves c_1 to c_4 increase r_3 with the increment 5mm in this order. | 27 |
| Figure 8: Fusee | 27 |
| Figure 9: Connection of a couple of non-circular pulleys by ropes through a spring | 28 |
| Figure 10: Profile of the groove in the coordinate system (X,Y) | 28 |
| Figure 11: Optimized relation between H and F. The curves (a) and (b) are the results of circular pulleys for the simple and complex mechanisms. The values of b are 18mm and 6.9mm, respectively. The curves (c) and (d) are the results of fusees of non-circular shape for the simple and complex mechanisms. The values (a,b) are (-0.69, 18.0) and (-0.60, 8.5), respectively. The curves (e) and (f) are the results of flat pulleys of non-circular shape for the simple and complex mechanisms. The values (a,b) are (-0.60, 17.25) and (-0.66, 8.5), respectively. | 29 |
| Figure 12: Overview of force measurement by the fabricated mechanism | 29 |
| Figure 13: Relationships between F versus H of the complex mechanism. Curves a and b are the calculated results relating to the circular and non-circular pulleys. Dot and cross marks are the experimental results relating to those pulleys, respectively. | 30 |
| Figure 14: Relationships between F versus H of the simple mechanism. Curves a and b are the calculated results relating to the circular and non-circular pulleys. Dot and cross marks are the experimental results relating to those pulleys, respectively. | 30 |
| Figure 15: Fabricated pulleys which are used to obtain the curve b in Fig. 13; (a) profile of the groove, (b) characteristics of the ρ versus G. | 31 |

List of Figures

| | |
|--|----|
| Figure 1: Basic mechanism for obtaining the stretch force | 24 |
| Figure 2: Various kinds of mechanisms for generating the force | 24 |
| Figure 3: Calculated results of the relation between H and F under such conditions that $h = r_0 = 100\text{mm}$, $k = 0.1\text{Kg/mm}$ and $30^\circ \leq \theta \leq 100^\circ$. The value of a in (b), (c), (d), (e) and (f) are $3/5r_0$, $2/5r_0$, $3/4r_0$, $1/6r_0$ and $2/3r_0$, respectively. Parameters b and c are $1/3r_0$ and $3/4r_0$. | 25 |
| Figure 4: Proposed mechanism for the force generation | 25 |
| Figure 5: Geometrical illustration for analyzing equilibrium of the mechanism in force | 26 |
| Figure 6: Calculated relation between H and F when circular pulleys are used in the complex mechanism under such conditions that $h = 95\text{mm}$, $r_0 = 35\text{mm}$, $r_1 = 7.5\text{mm}$, $r_2 = 5\text{mm}$, $L_0 = 19.05\text{mm}$, $k = 0.14\text{Kg/mm}$, $Q = 0.5\text{Kg}$ and $40^\circ \leq \theta \leq 100^\circ$. The curve c_0 is obtained under $r_3 = 0$. The curves c_1 to c_4 increase r_3 with the increment 2mm in this order. | 26 |
| Figure 7: Calculated relation between H and F when circular pulleys are used in the simple mechanism under the same conditions to those used in the complex mechanism. The curve c_0 is obtained under $r_3 = 0$. The curves c_1 to c_4 increase r_3 with the increment 5mm in this order. | 27 |
| Figure 8: Fusee | 27 |
| Figure 9: Connection of a couple of non-circular pulleys by ropes through a spring | 28 |
| Figure 10: Profile of the groove in the coordinate system (X,Y) | 28 |
| Figure 11: Optimized relation between H and F. The curves (a) and (b) are the results of circular pulleys for the simple and complex mechanisms. The values of b are 18mm and 6.9mm, respectively. The curves (c) and (d) are the results of fusees of non-circular shape for the simple and complex mechanisms. The values (a,b) are (-0.69, 18.0) and (-0.60, 8.5), respectively. The curves (e) and (f) are the results of flat pulleys of non-circular shape for the simple and complex mechanisms. The values (a,b) are (-0.60, 17.25) and (-0.66, 8.5), respectively. | 29 |
| Figure 12: Overview of force measurement by the fabricated mechanism | 29 |
| Figure 13: Relationships between F versus H of the complex mechanism. Curves a and b are the calculated results relating to the circular and non-circular pulleys. Dot and cross marks are the experimental results relating to those pulleys, respectively. | 30 |
| Figure 14: Relationships between F versus H of the simple mechanism. Curves a and b are the calculated results relating to the circular and non-circular pulleys. Dot and cross marks are the experimental results relating to those pulleys, respectively. | 30 |
| Figure 15: Fabricated pulleys which are used to obtain the curve b in Fig. 13; (a) profile of the groove, (b) characteristics of the ρ versus G. | 31 |

Abstract

A mechanism is described for achieving a desired force/motion relationship. The mechanism employs two hinged arms with pulleys and springs. In comparison to active force-control methods, the device is compact, energy saving, and robust. The device is ideally suited to miniature devices and, in a recent application, has been used in a mobile robot for inspecting pipes.

The relationship between the motion of the mechanism and its output force is analyzed using both analytical and approximate techniques to determine the optimum configuration and the dimensions of the various components. In the final design, experimental results demonstrate the superiority of non-circular eccentric pulleys over conventional pulleys for producing a specified force/motion curve.

1. Introduction

Coil springs are commonly used in force generating mechanisms when it is necessary to obtain a force that increases with the amount of extension or stretch. However, when the desired force is not directly proportional to the amount of extension, the force-generating mechanism must be modified [1]. Active servomechanisms may be used to control the spring extension, resulting in a constant force over a considerable distance. However, such methods make the force generating mechanism complex and costly. To avoid these difficulties, the concept of "force generation by using pulleys and springs" (FGPS) has been considered [2].

The original application for the mechanism described in this paper was a mobile robot for inspecting the inside of pipes. The robot presses against the pipe walls for traction and, ideally, the pressure should be independent of pipe diameter. Since the inspection robot must be quite small (small enough to fit in a pipe of 65mm inside diameter), it is important to find a constant-force mechanism that avoids the complexity of a servo system. Figure 4 illustrates the basic mechanism described in this paper. It consists of two arms hinged at one end to form a symmetric, collapsible structure. As the arms move apart, they drive two pulleys through intermediate gears. An extension spring is connected to cables that run between the two pulleys and resists the separating motion of the arms. Both circular and non-circular pulleys were considered for the device. The shape of the non-circular pulleys is adapted from a conical fusee as shown in Figure 8. The non-circular pulleys are designed so that the pulley radius can be expressed as a linear function of angular displacement. Analytical and approximate methods are discussed for deriving the desired relationship between the angle and pulley radius. Circular and non-circular pulleys have also fabricated and compared in experiments.

2. Description of Mechanism for Force Generation

Nomenclature:

| | |
|-----|---|
| A | vertex of mechanism |
| B | tip of left arm |
| C | tip of right arm |
| D | mechanism for pulling the arms together |
| F | force against rails m_1 and m_2 |
| H | height of mechanism |

| | |
|----------|---------------------------------------|
| h | length of arm, AB or AC, of mechanism |
| $m1, m2$ | rails supporting device |
| θ | angle between arms |

Figure 1 shows a simplified, two-dimensional schematic of the device riding between two rails, $m1$ and $m2$. A wheel is mounted at the lower tip of each arm and at the vertex, A, of the device. The goal is to construct a mechanism, D, that will pull the arms together, generating a force, F , that remains constant over a wide range of heights, H .

For the solution of this problem, six types of mechanisms, as shown in Figure 2, have been investigated. Dots in the figure show pivot joints which rotate freely. All of the mechanisms are symmetric with respect to the line bisecting the angle θ . For calculating the relation between the angle θ and force F , let us suppose that two ends of each spring connect directly to free joints. Also, let k stand for the elasticity of a spring and L_0 for the length of the spring in a no-load condition. Note that the mechanism is in equilibrium when the sum of the moments about any point in the system is zero. The relation between the angle, θ , and force, F , of each mechanism is obtained as shown in Appendix A, using the partial length r_0 of the two arms and the lengths a , b , and c of subsidiary links in Figure 2.

Figure 3 shows the calculated results of the relation between the distance $H = h \cos(\theta/2)$ and force, F , of the linkage types in Figure 1 when the springs are all the same in elasticity. It is observed from the figure that for most structures the force, F , increases as the distance H decreases. However, in the curves (a), (c), and (e) the force tends to decrease as the distance becomes small. A large change of the value of F is observed in the curves (a), (d), and (f). The incompleteness of the curves (d) and (f) is due to motional limitations of the linkages. We can see that none of the six curves is linear. The curve (e) is the most linear of the six, and thus, the mechanism in Figure 2(e) is considered to be the most appropriate to produce a constant force for a range of angles θ . However, the mechanism is too complex for actual use. In general we observe that the spring stretches too much to keep the force F constant. This is caused by the fact that the ends of the spring are connected directly to points on the linkages. For better results, the ends of the spring could be connected to a body with an adjustable position or length,

instead of a fixed body. Therefore, we will consider the modified mechanisms in the following section.

3. Force Generation by Using Pulleys and Spring

Based on the considerations in Section 2, we have devised a linkage for the constant force device. In the following section, I will explain how it works, and then analyze the force members of the mechanism to find out relation of the angle between the two arms and the stretch force. The shape of the pulleys is circular in this section.

3.1. Link Mechanism

Figure 4 shows the proposed link mechanism for force generation. Two arms AB and AC connect the ends of two subsidiary links at points D_1 and D_2 at a distance $r_{\tilde{v}}$ from the point A. The other ends of the links are put together to make a joint J. The partial links AD_1 , AD_2 , and subsidiary links JD_1 , JD_2 are connected with each other using pivot joints with rotational axes perpendicular to the plane in which the two arms rotate. Therefore, the links compose a four-bar linkage mechanism A- D_1 -J- D_2 . Since the four links are of equal length, the four points A, D_1 , J, and D_2 make a rhombus. The gear G_1 located at the point D_1 is fixed to the link JD_1 , but rotates with respect to link AB. Similarly, the gear G_2 located at the point D_2 is fixed to the link JD_2 , but rotates with respect to link AC. Therefore, two gears G_1 and G_2 rotate about their axes at points D_1 and D_2 , with the links JD_1 and JD_2 , respectively. The gears G_1 and G_2 drive the pulleys P_1 and P_2 through the gears G_3 and G_4 . An extension spring, S, joins the two ropes. The other ends of the ropes are wound around the pulleys P_1 and P_2 . The rotational motions of the pulleys adjust to the length of the spring for an optimum tensile force.

If it is required to attach the pulleys P_1 and P_2 on the links AD_1 and AD_2 , the gears G_1 and G_2 would be fixed to the links AD_1 and AD_2 , respectively. Depending on the desired relation between the distance H and Force F , we can omit the gears G_3 and G_4 and replace the gears G_1 and G_2 by the pulleys P_1 and P_2 , respectively. That is, the centers of the pulleys are attached to the points D_1 and D_2 . We will call such an arrangement a "simple mechanism", while the arrangement in Figure 4 becomes a "complex mechanism". The major difference between the mechanism in Figure 4 and the one in Figure 2 is that the

ends of the spring are wound round the pulleys, using flexible ropes. Two of the links of the four-bar linkage are actually sections of the two arms. No other links are required for the mechanism in Figure 4.

3.2. Analyses of Motion and Force Members of the Mechanism

The mechanism in Figure 4 is valid only if the spring extends as the angle θ increases. It must now be determined whether the spring actually extends when the two arms open. Therefore, we develop the relation between the angle θ and the length of the spring as follows. Let the radii of the gears G_1 and G_2 be r_1 , and those of gears G_3 and G_4 be r_2 . Also, let the radii of the pulleys P_1 and P_2 be r_3 . Now let M be the minimum length of the rope connecting the pulley with the end of the spring, and W be the length of the rope around a pulley. The length W depends on the number of turns around the pulley. Hence, the total length between the two points where the ends of the ropes meet the pulleys is $2M+L$, where L is the variable length of the spring. We subtract the length, $2(r_0 - r_1 + r_1 \sin(\theta/2))$ between the centers of the two pulleys from the total length, $2M+L$, to calculate the length of the rope which is wound round the pulleys P_1 and P_2 .

$$2M+L=2(r_0+r_1+r_2)\sin(\theta/2)+\frac{2(2\pi-\theta)r_1r_3}{r_2}+2r_3(2\pi-\theta/2)+2W \quad (1)$$

We then differentiate L in equation (1) by θ to yield

$$\frac{dL}{d\theta}=(r_0+r_1+r_2)\cos(\theta/2)-r_3(1+2\frac{r_1}{r_2}) \quad (2)$$

The equation implies that the value of L becomes large as the angle θ increases when the value of $dL/d\theta$ is positive. In most cases, the value is positive since the values of r_1 , r_2 , and r_3 are smaller than that of r_0 . The spring must extend to give a large force when the two arms open.

We analyze the relation between the angle θ and force F in Figure 4, illustrating the force. The force components are exerted on each link of the mechanism. Let T denote the output force of the spring S , then the gear G_1 is driven by the force T_1 .

$$T_0 = \frac{r_3}{r_2} T. \quad (3)$$

The compression force, U , exerted on the link JD_1 is obtained by setting the moment about the point D_1 to zero.

$$U = \frac{2r_1 T_0}{r_0 \sin \theta}. \quad (4)$$

Expressing the moment about the point A for arm AB gives

$$\{(r_0 + r_1 + r_2) \cos(\theta/2) - r_3\} T = \frac{hF}{2} \sin(\theta/2) + r_0 U \sin \theta. \quad (5)$$

Equations (3), (4), and (5) are combined to give

$$F = \frac{2T \{(r_0 + r_1 + r_2) \cos(\theta/2) - r_3 (1 + 2r_1/r_2)\}}{h \cdot \sin(\theta/2)}. \quad (6)$$

Figure 5 shows a geometrical illustration of the mechanism for two different values of θ . The symbol θ_{min} denotes the minimum value of θ . When the angle between the links is θ , the link JD_1 is inclined by an amount $\gamma = \theta - \theta_{min}$, and the pulley rotates by $\delta = (\theta - \theta_{min})/2$. When the links are separated by the angle, θ_{min} , the pulley P_1 is rotated by ϕ with respect to the initial configuration; i.e., the total angular shifts of the pulley is given by

$$\phi = \delta + \frac{r_1}{r_2} \gamma = \left(0.5 + \frac{r_1}{r_2}\right) (\theta - \theta_{min}). \quad (7)$$

Suppose L_{min} expresses the length of the spring when $\theta = \theta_{min}$, then we have

$$L = 2(r_0 + r_1 + r_2) \sin(\theta/2) - \xi - \eta_1 - \eta_2, \quad (8)$$

where

$$\xi = 2(r_0 + r_1 + r_2) \sin(\theta_{min}/2) - L_{min}, \quad (9)$$

$$\eta_1 = \phi r_3, \quad (10)$$

$$\eta_2 = \eta_1. \quad (11)$$

ξ is the length of the rope connecting the spring and two pulleys when $\theta = \theta_{min}$. η_1 and η_2 are the lengths of the ropes which unwind from the pulleys P_1 and P_2 , respectively. When two arms intersect with the angle θ_{min} , we can express the length L_{min} by $\epsilon_o L_0$, where ϵ_o is a constant greater than 1. The force T is written as

$$\begin{aligned} T &= k(L - L_0); \\ &= k [2(r_0 + r_1 + r_2) \{ \sin(\theta/2) - \sin(\theta_{min}/2) \} + L_0(\epsilon_o - 1) - 2r_3\phi]. \end{aligned} \quad (12)$$

We obtain the final form by inserting equation (12) into equation (6)

$$\begin{aligned} F &= 2k [2(r_0 + r_1 + r_2) \{ \sin(\theta/2) - \sin(\theta_{min}/2) \} + L_0(\epsilon_o - 1) - 2r_3\phi] \\ &\quad \times [(r_0 + r_1 + r_2) \cos(\theta/2) - r_3(1 + 2\frac{r_1}{r_2})] \frac{1}{h \cdot \sin(\theta/2)}. \end{aligned} \quad (13)$$

In the case that the pulleys are attached on the subsidiary links or arms of the scissors structure, Equation (13) should be modified by replacing $(r_0 + r_1 + r_2)$ with $(r_0 - r_1 - r_2)$.

3.3. Relationship Between Force and Deformation of the Mechanism

By using the equation(13), we obtain the relation between the distance H and force F , since the value of ϵ_0 can be used to make the force F equal to the ideal force Q when θ is θ_{min} . First, we consider the "simple mechanism" which uses only the pulleys. In this case, r_1 and r_2 are zero. Therefore, Equation (13) is simplified as

$$F = \frac{2k[2r_0\{\sin(\theta/2) - \sin(\theta_{min}/2)\} + L_0(\epsilon_0 - 1) - 2r_3\phi] \times [r_0\cos(\theta/2) - r_3]}{h \cdot \sin(\theta/2)}, \quad (14)$$

where

$$\phi = (\theta - \theta_{min})/2. \quad (15)$$

Equation (14) is also valid for the simple mechanism having no subsidiary links; that is, when pulleys are fixed on the two arms.

Figure 6 shows the calculated results of the relation between H and F depending on radius of the pulleys in a complex mechanism combining pulleys and gears as shown in Figure 4. For instance, the curve c_3 is obtained when $r_3 = 6$ mm. Figure 7 shows the results of the relation between H and F in a simple mechanism having no gears. In this case, equation (13) applies, with $r_1 = r_2 = 0$. The curve c_3 shows the result for a pulley of 15 mm radius. It is evident that the curve c_0 changes the force F remarkably. Since no pulleys are considered, the curve corresponds to that in Figure 3 (a).

By comparing the results of the relation between H and F for the complex mechanism with those of the simple mechanism, it is evident that the value of r_3 is smaller than that of the simple mechanism for the same amount of force. Also, the shape of the curves is smoother than that of the simple mechanism. Based on these facts, a combination of pulleys and gears is desirable. The curves in Figure 6 and Figure 7 imply that it is difficult to make the force F constant over a wide range of the distance H . However, we can see intuitively that there is an appropriate curve between the curves c_3 and c_4 that will produce a force roughly equal to the ideal force Q . We discuss optimization methods in

the following section to determine dimensions for the pulleys that will result in an appropriate curve.

4. Optimization of Force Generation Mechanism

The force generation mechanism, or more specifically the dimensions of the pulleys, should be exactly determined to adjust the length of the spring for generating the force we wish. We consider two types of pulleys: One is a circular pulley which is commonly used. The other is an eccentric non-circular pulley. In the "complex mechanism," the parameters r_1 and r_2 also affect the characteristics of the force generation. However, these are out of the scope of this paper. In determining the dimensions of the pulleys, we propose analytical and approximate methods. Optimization of the spring elasticity is also discussed, once the parameters of the pulleys are given.

4.1. Analytical Method

The force F is calculated from equation (13). At this point, we express the radius r_3 by the term $r(\rho)$ defining the relation between the radius of the pulley and its angular shift ρ . The force F is given by

$$F=2k[2(r_0+r_1+r_2)\{\sin(\theta/2)-\sin(\theta_{min}/2)\}+L_0(\epsilon_0-1)-2G] \\ \times [(r_0+r_1+r_2)\cos(\theta/2)-r(\rho)(1+2\frac{r_1}{r_2})] \frac{1}{h \cdot \sin(\theta/2)}, \quad (16)$$

where G stands for the term expressing the circumference of the pulley which rotates as θ increases from θ_{min} . In this paper, we consider a pulley for which the relation between the pulley radius r and angular shift ρ is linearly expressed as

$$r(\rho)=2a\rho+b. \quad (17)$$

The parameters, a and b , are adjusted to determine the shape of the pulley. Evidently, the value of b is positive and that of a is zero when the pulley is circular. In such a case if the

to

pulley radius is expressed by equation (17), we have the following relations for Q_j

$$\int_0^\phi r(\rho) d\rho; \\ = a\phi^2 + b\phi, \tag{18}$$

and

$$r(\rho) = 2acj + b, \tag{19}$$

where $\langle j \rangle$ is determined from equation (7). Therefore, equation (16) is written by the expression

$$F = 2k\{2(r_0 + r_1 + r_2)\{\sin(\theta/2) - \sin(\theta_{min}/2)\} + L_0(\epsilon_0 - 1) - 2(a\phi^2 + b\phi)\} \\ \times \frac{[(r_0 + r_1 + r_2)\cos(e/2) - (2acj + b)(l + 2^{\wedge} \rho)]}{z} \frac{1}{h \cdot s \cdot \sqrt{Q/2y}} \tag{20}$$

Now we look for a function giving the ideal value, Q for F such that

$$Q = f(\theta) \tag{21}$$

Then, we define the error function $E9$ by the relation

$$EQ = \{F9 - Q0\}^2. \tag{22}$$

The values of a and b are determined by making the value of EO minimum in the range of θ . That is, to minimize the value calculated by

$$Z = \int_0^{\theta_{min}} E\theta d\theta. \quad (23)$$

Since the expression of $E\theta$ is decomposed into the terms $\theta^p \sin^m \theta \cos^n \theta$ (p, m, n are positive integers), the integration in equation (23) can be performed and expressed in terms of a and b (see Appendix B for detailed calculation). By differentiating the function Z with respect to a and b and equating them to zero, we have two equations with unknown parameters a and b . It is not easy to solve such simultaneous equations in general. However, we notice that we can assign the value of the parameter b . Also, the parameter ϵ_0 should be given by considering the initial condition $\theta = \theta_{min}$ ($\rho=0, \phi=0$), where the value of F is $Q_0 = f(\theta_{min})$. Therefore, from equation (20)

$$\epsilon_0 = \frac{hQ_0 \sin(\theta_{min}/2)}{2kL_0 \{(r_0 + r_1 + r_2) \cos(\theta_{min}/2) - b(1 + 2r_1/r_2)\} + 1}. \quad (24)$$

Then, we can determine the value of a by solving a cubic equation.

When the shape of the pulley is circular, the calculation process is simple, since the value of a is zero and we can determine the value of b by solving the equation obtained by differentiating the function Z in equation (23) with respect to b . The knowledge of b is useful in the calculation of a . We can recommend that the optimum radius of the circular pulley be found first, so that the parameter a for the non-circular pulley can be calculated by using the value of b .

4.2. Approximate Method

We can determine the optimum dimension of the pulley also by using the Least Square Method (LSM), as long as the change of the radius of the pulley as a function of angular displacement is smooth. Let Q_j denote the ideal value of F when $\theta = \theta_j$, then we have the following expression from equation (20) since the equations (19) and (24) are valid:

$$\begin{aligned}
F_j = & 2k [2(r_0 + r_1 + r_2) \{ \sin(\theta_j/2) - \sin(\theta_{min}/2) \} + J - 2(a\phi_j^2 + b\phi_j)] \\
& \times \left[(r_0 + r_1 + r_2) \cos(\theta_j/2) - (2a\phi_j + b) \left(1 + 2\frac{r_1}{r_2} \right) \right] \frac{1}{h \cdot \sin(\theta_j/2)},
\end{aligned} \tag{25}$$

where J is the term of $L_0(\epsilon_0 - 1)$ which is written as

$$J = \frac{hQ_0 \sin(\theta_{min}/2)}{2k \{ (r_0 + r_1 + r_2) \cos(\theta_{min}/2) - b(1 + 2r_1/r_2) \}} \tag{26}$$

and

$$\phi_j = \left(0.5 + \frac{r_1}{r_2} \right) (\theta_j - \theta_{min}). \tag{27}$$

Subtracting F_j from the ideal value Q_j and squaring the result given the absolute error Z .

$$Z = \sum_j (F_j - Q_j)^2 \tag{28}$$

Several sets of data are used to make the force as close to the ideal force as possible. After summing the terms obtained by using these actual data, we differentiate the summation, Z , with the parameters a and b . Since the procedures are similar to those described in Section 4.1, we can determine the values of a and b , by setting the results of the differentiation zero, to make the error minimum. When the pulley is circular, the value of a is zero and we can solve for the unknown parameter b

$$\Sigma U_{1j} b^3 + \Sigma U_{2j} b^2 + \Sigma U_{3j} b + \Sigma U_{4j} = 0$$

(29)

The terms $U_{1j} \dots U_{4j}$ are shown in Appendix C.

When the pulley is eccentric and non-circular, we can assign a value for b . It is recommended to use the solution of a circular pulley for the assignment so that the value of a can be obtained by solving a cubic equation.

$$\Sigma S_{1j} a^3 + \Sigma S_{2j} a^2 + \Sigma S_{3j} a + \Sigma S_{4j} = 0. \quad (30)$$

The terms $S_{1j} \dots S_{4j}$ are shown in Appendix D.

As long as the shape of the pulley is smooth, the spring retracts or extends as the rope winds in a spiral around the pulley. If the effective angular range exceeds $2\pi(\text{rad})$, the rope can turn many times around the pulley by extending the pulley groove to form a fusee as shown in Figure 8. The shift of the groove along the axis of the fusee will be negligible when the effective angular range is less than $2\pi(\text{rad})$. In this case, we can make flat pulleys of non-circular-shape by interpolating radii along the pulley so that the groove makes a single smooth loop.

Figure 9 shows the rope connecting two non-circular pulleys P_1 and P_2 . The thick curve is the effective groove radius and the broken curve is for the extension of the curve for a fusee. For a fusee, the rope detaches from points u_1 and u_2 since the groove is not in one plane. For flat pulleys, the rope detaches from points v_1 and v_2 . The length between the points v_1 and v_2 is not equal to the length between the two rotational centers (i.e., E_1 and E_2) of the fusee, regardless of the sign of the parameter a . Since the equation (25) is no longer applicable we consider a formula for the dimensions of the flat pulleys below.

Let λ denote the angle between the line connecting points E_1 and u_1 and the line connecting points E_1 and v_1 . Also, let ω denote positional displacement as shown in Figure 9. Figure 10 reveals a method for calculating the distance r_3 and the displacement ω . The

profile of the groove is written in the coordinate system (X, Y) as

$$X^2 + Y^2 = \{2a\phi + b - 2a \tan^{-1}(Y/X)\}^2. \quad (31)$$

If the value of a is small enough we can approximate that

$$\tan^{-1}(Y/X) \approx Y/X. \quad (32)$$

Inserting equation (32) into equation (31), and letting the value of the differential dY/dX approach infinity, we have

$$\lambda = \tan^{-1} \frac{-2a}{2a\phi + b}, \quad (33)$$

$$r_3 = \sqrt{4a^2 + (2a\phi + b)^2}. \quad (34)$$

Given an initial condition, such as $\phi = 0$, it is evident that r_3 is equal to b when a is less than or equal to zero. Equation (34) is valid when a is positive. Then, we define r_{30} for the value of r_3 in the initial condition.

$$r_{30} = \begin{cases} b, & a \leq 0 \\ \sqrt{4a^2 + b^2}, & a > 0 \end{cases} \quad (35)$$

It follows that

$$\omega = r_3 \tan \lambda. \quad (36)$$

The values of λ and ω are positive when a is positive, and vice versa. Following the procedure of equation (25), we obtain the following expression for the force $F \#$:

$$F_j = 2k [2(r_0 + r_1 + r_2) \{ \sin(\theta_j/2) - \sin(\theta_{min}/2) \} + J - 2 \{ a(\phi_j - \lambda_j)^2 + b(\phi_j - \lambda_j) \} - 2\omega_j] \\ \times [(r_0 + r_1 + r_2) \cos(\theta_j/2) - r_{30} (1 + 2 \frac{r_1}{r_2})] \frac{1}{h \cdot \sin(\theta_j/2)}, \quad (37)$$

where

$$J = \frac{hQ_0 \sin(\theta_{min}/2)}{2k \{ (r_0 + r_1 + r_2) \cos(\theta_{min}/2) - r_{30} (1 + 2r_1/r_2) \}}. \quad (38)$$

By assigning an appropriate value to b , the value of r_{30} is given by equation (35). Then assuming a small value for a , we can obtain the force F_j from equation (37) and determine the error Z by evaluating equation (28). The form of Z is too complicated to differentiate with respect to a and b . As a result, it is difficult to find a unique value of unknown parameters a and b . To find out the most appropriate value of a for making the value of Z minimum, we can check the value of Z by adding or subtracting a little to zero. Although this process is tedious, we can obtain the optimum value.

If the dimensions of the pulleys are given, we can optimize the force generation mechanism by selecting an appropriate elasticity for the spring. It is easy to extract the form to determine the elasticity since equations (25) and (37) expressing the force F include only the term k . That is, we subtract equation (25) or (37) from the ideal value Q_j and square the result to determine the absolute error Z in equation (28). Several sets of data are used to make the force as close to the ideal force as possible. After summing up the terms which are obtained using actual data, the summation is differentiated with respect to k . Equating the results of the differentiation to zero, so that the error becomes minimum, we can determine the elasticity, k , of the spring.

5. Design of Pulleys and Experimental Results

The dimensions of the pulleys are calculated using either the analytical or the approximate method. After determining optimum shapes for circular pulleys, and eccentric non-circular pulleys, in the simple and complex mechanisms under the conditions that Q is constant and equations (17) and (24) are valid, the results of the optimization are compared to find out which is most accurate. Experimental results are given for the relation between the distance, H , and force, F , to verify the validity of the optimization.

5.1. Circular Pulley

We take the condition in equation (24) into consideration and use equation (25). When the shape of the pulley has a circular form, the value of a is zero and the radius b is obtained by solving a cubic equation. Figure 11 shows the results of the relation between the distance H and Force F when $Q = 0.5$ Kg. Results for the circular pulleys in simple and complex mechanisms are shown by curves (a) and (b). The force from the complex mechanism comes closer to the ideal force, Q , than that from the simple mechanism.

5.2- Fusee

Circular pulleys can be used to produce a force, F , which is nearly equal to the indicated force Q . However, the curve expressing the relation between the distance H and Force F is not similar to the curve indicated by the function in equation (21). In fact, the curves (a) and (b) in Figure 11 are not satisfactory to determine a constant force over wide ranges of H . Therefore, we have to consider pulleys of non-circular-shape. The dimensions of the fusees are determined by finding the parameters a and b which make the value of Z in equation (28) minimum. We suppose that the displacement of the groove along the axis of the pulley is small enough to be neglected. Figure 11 (c) shows the result of the relation between the distance H and Force F of the pulley for the simple mechanism and Figure 11 (d) shows the result for the complex mechanism. It is evident that not only the force but also the shape of the curve becomes similar to that of the curve given by the function Q . The curve (d) is almost parallel to the horizontal axis.

5.3. Flat Pulleys of Non-Circular-Shape

We designed flat pulleys having eccentric non-circular shapes by using the iterative method which was discussed in the latter half of Section 4.2. The curve in Figure 11 (e) shows the results of the relationship between the distance l and force F for the simple mechanism. Figure 11 (f) shows the result for the complex mechanism. The shapes of these curves are found to be similar to those of the fuseses.

5.4. Experimental Results

In the actual design, the size of the pulley is an important factor. Since the size of the pulley in the simple mechanism tends to become large, the complex mechanism is recommended to keep the force generation mechanism compact. In addition, a mechanism that has a large value of $r_1 + r_2$ and a smaller value of r_1/r_2 is recommended for obtaining a large force F . However, smallness of r_1/r_2 makes r_1 large and prevents fabrication of compact device for the force generation. Therefore, a complex mechanism was adopted for the equipment shown in Figure 12. The physical dimensions of the mechanism are $l=0.14\text{Kg/mm}$, $l_i=95\text{mm}$, $r_Q=35\text{mm}$, $r_1=1.5\text{mm}$, $r_2=5\text{mm}$, $Q_j=0.5\text{Kg}$, $40^\circ \sim 100^\circ$. For these dimensions, circular pulleys and flat pulleys of non-circular-shape were made.

The circular pulleys have a diameter of $\phi=6.9\text{mm}$. The curve (a) in Figure 13 shows the calculated relation between H and F , and dots show the experimental data for the circular pulley used with the complex system. The optimized parameters of the flat pulley of non-circular-shape are $a=-0.66$ and $b=8.5\text{mm}$. These values are obtained by considering the position where the rope detaches from the groove of the flat pulley. The curve (b) in Figure 13 shows the calculated result and the cross marks show the measured result. The curves (a) and (b) in Figure 13 correspond to those of (b) and (f) in Figure 11, respectively. The relationship between H and F for the simple mechanism are shown in Figure 14. The curves (a) and (b) in Figure 14 correspond to those of (a) and (e) in Figure 11, respectively. The fact that the calculated and measured results are close indicates that the analysis for calculating the force F are valid. We can confirm that the eccentric non-circular shape in the flat pulley makes it possible to generate a force closer to the designated force Q , than the pulley of circular shape can achieve.

Figure 15 illustrates a profile of the groove and the characteristics of the p versus G of

the flat pulley. The pulley is effective only in the range $0^\circ \leq \phi \leq 120^\circ$ for which case $40^\circ \leq \theta \leq 100^\circ$. The radii of the unused area of the pulley are interpolated so that the shape of the pulley becomes smooth. The profile of the groove and the characteristics of ρ versus G for the fuseses are almost the same as those of the flat pulleys.

The result of the approximate method is almost the same as that of the analytical method when the curve expressing the function $f(\theta)$ is smooth. Thus, in a case where the value of Q is constant, the approximate method is shown to be effective for practical use in reducing the amount of computation.

6. Conclusion

The design and optimization of a force generating mechanism have been discussed. The mechanism has been applied to a mobile robot for inspecting pipes that vary between 90 mm and 120 mm in diameter [3]. A major advantage to the mechanism is that it makes servo control unnecessary. The mechanism uses an extension spring and a pair of specially designed pulleys to achieve a desired force/motion trajectory. As the mechanism opens and closes, (adapting to the inside diameter of the pipe) a linkage drives a pair of gears which rotate a pair of pulleys. The pulleys are designed with a non-circular shape. As they rotate, they stretch an extension spring. The rate of extension is determined so that the mechanism exerts a nearly constant force against the inner walls of the pipe. Exact and approximate methods are considered for determining the optimum relationship between pulley radius and angle of rotation. The approximate methods can be used effectively as long as the desired force/motion relationship is a smoothly varying function. In the final design, the pulleys are driven by intermediate gears which permit the use of smaller pulley diameters.

Acknowledgments

The author thanks Takeo Kanade for his support and encouragement during his stay at the Robotics Institute to make this study. Also, he thanks Donald Schmitz, Edward C. Kurtz, and Brad Barcic for providing invaluable advice during the design, construction, and experiment of the two-hinged arms with pulleys and spring, and Mark R. Cutkosky for his helpful discussion and reviewing.

References

- [1] Chironis, N. P., 1966, *Mechanisms, Linkages, and Mechanical Controls*. New York: McGraw-Hill.
- [2] Okada, T., 1984 (Aug.), "Optimization of Mechanisms for Force Generation by Using Pulleys and Spring." Paper delivered at the Int. Symp. Robotics Res. Kyoto, Japan.
- ✓ [3] Okada, T., and Kanade, T. (1985), "Three-Wheeled Self-Adjusting Vehicle in Pipe, FERRET-1", Technical Report, Carnegie-Mellon University, Pittsburgh, Pa. (in preparation).

Appendix A

Relations between F and θ are as follows:

(a)

$$F = \frac{2kr_0}{h}(L-L_0)\cot\left(\frac{\theta}{2}\right) \quad \text{where} \quad L = 2r_0\sin(\theta/2).$$

(b)

$$F = \frac{2kar_0}{hL}(L-L_0), \quad \text{where} \quad L = \{r_0^2 - 2ar_0\cos(\theta/2) + a^2\}^{1/2}.$$

(c)

$$F = \frac{8ka^2}{hL}(L-L_0)\cos\left(\frac{\theta}{2}\right), \quad \text{where} \quad L = \{r_0^2 - 4a(r_0-a)\cos^2(\theta/2)\}^{1/2}.$$

(d)

$$F = \frac{kr_0L(L-L_0)}{ah\{p\cos(\theta/2) - q\sin(\theta/2)\}}, \quad \text{where} \quad L = r_0\cos(\theta/2) - \{a^2 - r_0^2\sin^2(\theta/2)\}^{1/2},$$

$$p = \frac{(a^2 + r_0^2 - L^2)}{(2ar_0)} \quad \text{and} \quad q = \frac{L}{a\sin(\theta/2)}.$$

(e)

$$F = \frac{kr_0}{h}(L-L_0)\cot(\theta/2), \quad \text{where} \quad L = (r_0 - 2a)\sin(\theta/2).$$

(f)

$$F = \frac{k(L-L_0)}{h} \left\{ \frac{r_0^2}{p}\cos(\theta/2) - r_0 + \frac{(r_0-c)^2}{q} \right\}, \quad \text{where} \quad p = \{a^2 + n - r_0\sin^2(\theta/2)\}^{1/2},$$

$$q = \{b^2 - (r_0-c)^2\sin^2(\theta/2)\}^{1/2}, \quad L = r_0\cos(\theta/2) - (r_0-c)\cos(\theta/2) - p - q.$$

Appendix B

Denote $\int_0^{\pi} \rho^p \sin^m \theta \cos^n \theta d\theta$ by $I[m, n, p]$.

When $m \geq 1$ and $n \geq 1$,

$$I[m, n, p] = \{ \theta^{p-1} \sin^m \theta \cos^{n-1} \theta [p \cos \theta + (m+n) \theta \sin \theta] + (n-1)(m+n) I[m, n-2, p] \\ - mp I[m-1, n-1, p-1] - p(p-1) I[m, n, p-2] \} / (m+n)^2.$$

When $m \geq 1$ and $n=0$,

$$I[m, 0, p] = \{ \theta^{p-1} \sin^{m-1} \theta [p \sin \theta - m \theta \cos \theta] \\ + m(m-1) I[m-2, 0, p] - p(p-1) I[m, 0, p-2] \} / m^2.$$

Appendix C

Let the symbols $g_1, g_2, g_3, g_4, g_5,$ and g_6 express the following terms.

$$g_1 = 2(r_0 + r_1 + r_2) \{ \sin(\theta/2) - \sin(\theta_{min}/2) \}$$

$$g_2 = hQ_0 / (2k) \sin(\theta_{min}/2)$$

$$g_3 = (r_0 + r_1 + r_2) \cos(\theta_{min}/2)$$

$$g_4 = (r_0 + r_1 + r_2) \cos(\theta/2)$$

$$g_5 = 1 + 2r_1/r_2$$

$$g_6 = 2k/h / \sin(\theta/2)$$

Then, we have

$$U_1 = -2g_5^2 g_6 \phi$$

$$U_2 = g_6 \{ g_1 g_5^2 + 2\phi(g_3 g_5 + g_4 g_5) \}$$

$$U_3 = - \{ g_4 g_6 (g_1 g_5 + 2g_3 \phi) + g_5 g_6 q_1 - Q g_5 \}$$

$$U_4 = g_4 g_6 q_1 - Q g_3$$

where

$$q_1 = g_1 g_3 + g_2.$$

Appendix D

Let the symbols $g_1, g_2, g_3, g_4, g_5,$ and g_6 have the similar expressions as shown in Appendix C. Then, we have

$$S_1 = 16g_5^2 g_6 \phi^5$$

$$S_2 = -12g_5 g_6 \phi^3 q_1$$

$$S_3 = 2\phi \{g_5(g_5 g_6 q_1^2 - 2Q\phi) + g_6 q_2 \phi (4g_5 q_1 + \phi q_2)\}$$

$$S_4 = q_3(Q - g_6 q_1 q_2)$$

where

$$q_1 = g_1 + g_2 / (g_3 - b g_5) - 2b\phi$$

$$q_2 = g_4 - b g_5$$

$$q_3 = \phi q_2 + g_5 q_1.$$

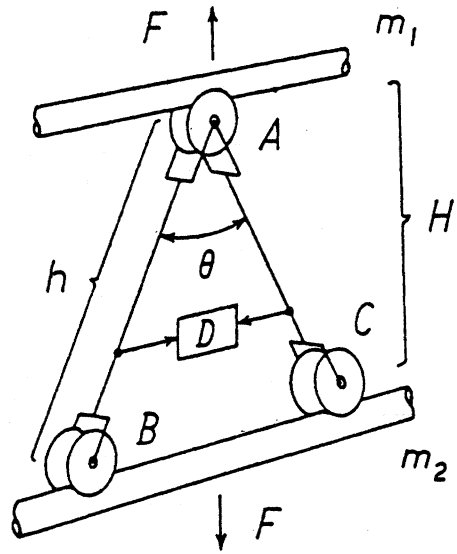


Figure 1: Basic mechanism for obtaining the stretch force

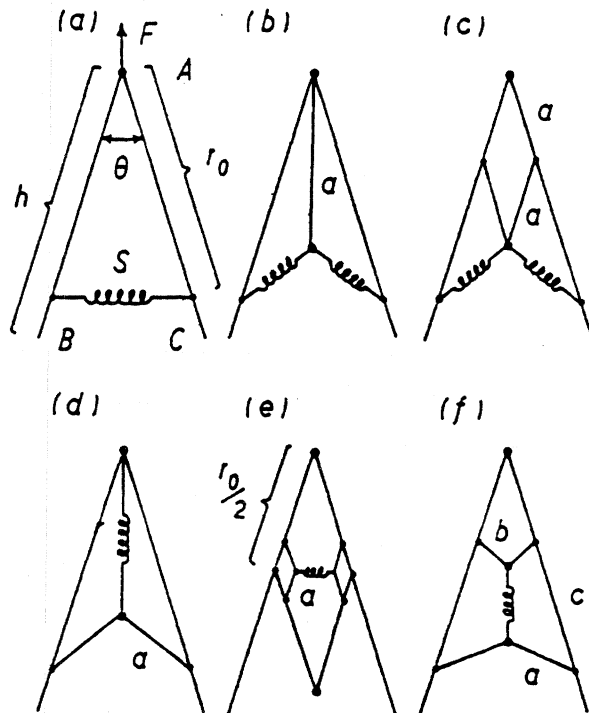


Figure 2: Various kinds of mechanisms for generating the force

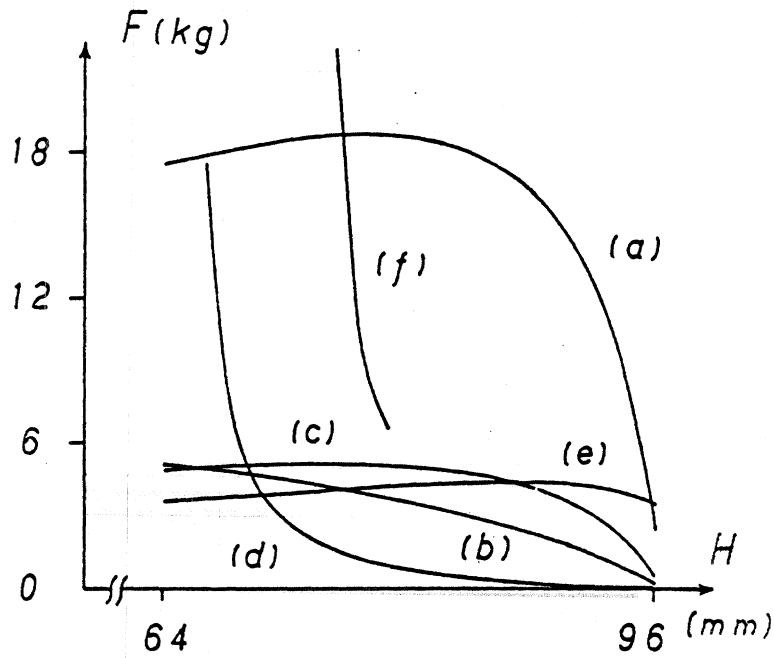


Figure 3: Calculated results of the relation between H and F under such conditions that $h = r_0 = 100\text{mm}$, $k = 0.1\text{Kg/mm}$ and $30^\circ \leq \theta \leq 100^\circ$. The value of a in (b), (c), (d), (e) and (f) are $3/5r_0$, $2/5r_0$, $3/4r_0$, $1/6r_0$ and $2/3r_0$, respectively. Parameters b and c are $1/3r_0$ and $3/4r_0$.

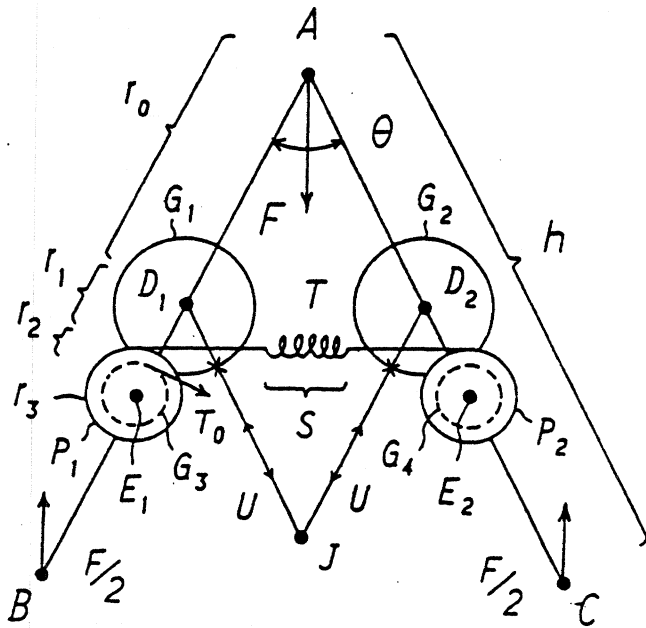


Figure 4: Proposed mechanism for the force generation

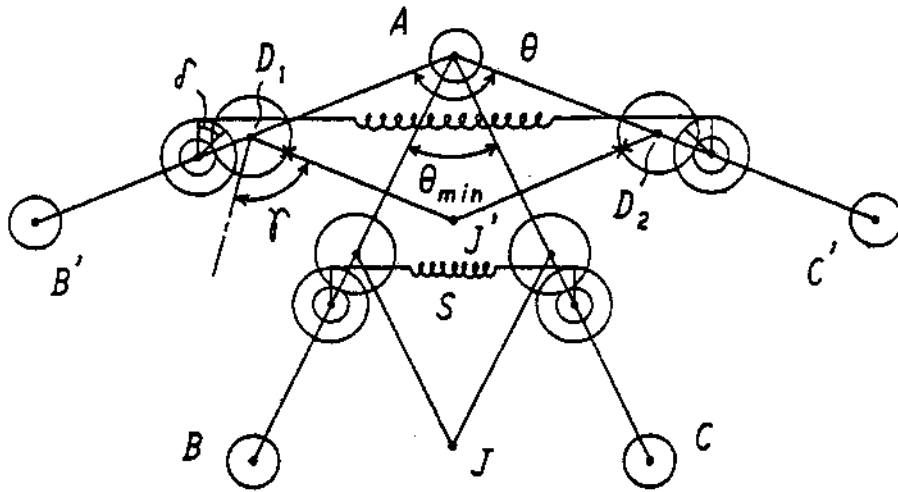


Figure 5: Geometrical illustration for analyzing equilibrium of the mechanism in force

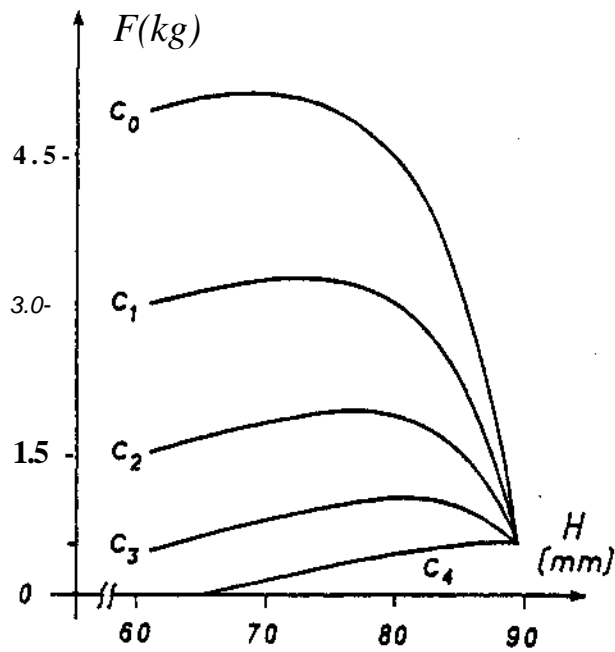


Figure 6: Calculated relation between H and F when circular pulleys are used in the complex mechanism under such conditions that $h = 95\text{mm}$, $r_Q = 35\text{mm}$, $r_1 = 7.5\text{mm}$, $r_2 = 5\text{mm}$, $L_Q = 19.05\text{mm}$, $k = 0.14\text{Kg/mm}$, $Q \cdot 0.5! < g$ and $40^\circ \leq \theta \leq 100^\circ$. The curve c_0 is obtained under $x_n = 0$. The curves c_1 to c_4 increase r^{\wedge} with the increment 2mm in this order.

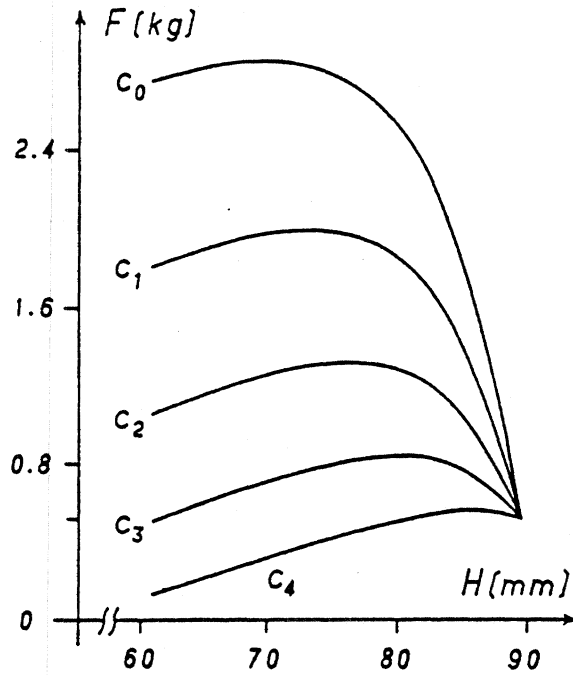


Figure 7: Calculated relation between H and F when circular pulleys are used in the simple mechanism under the same conditions to those used in the complex mechanism. The curve c_0 is obtained under $r_3 = 0$. The curves c_1 to c_4 increase r_3 with the increment 5mm in this order.

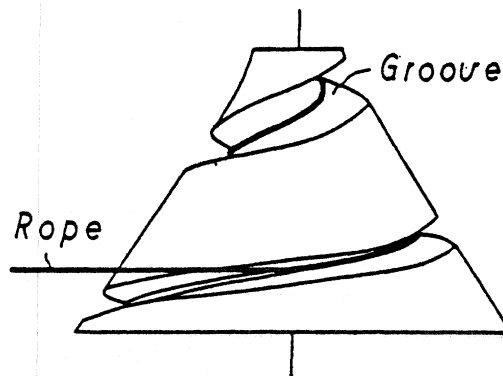


Figure 8: Fusee

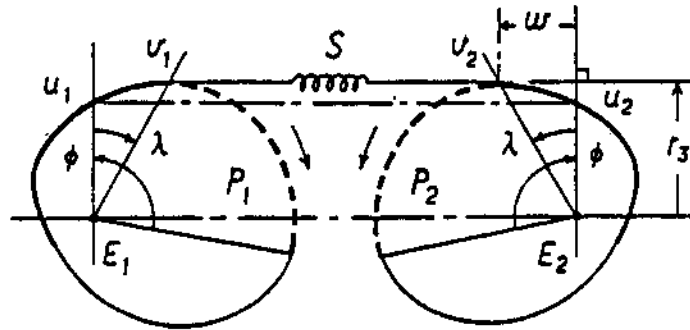


Figure 9: Connection of a couple of non-circular pulleys by ropes through a spring

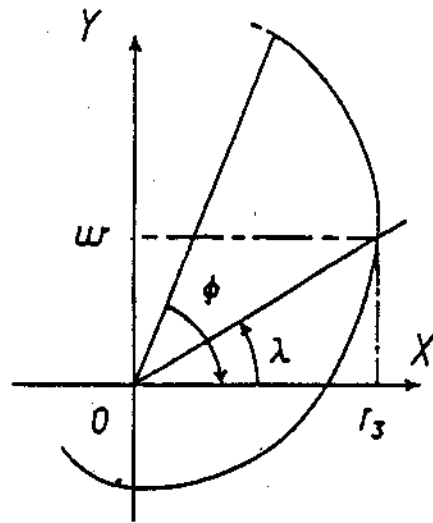


Figure 10: Profile of the groove in the coordinate system (X,Y)

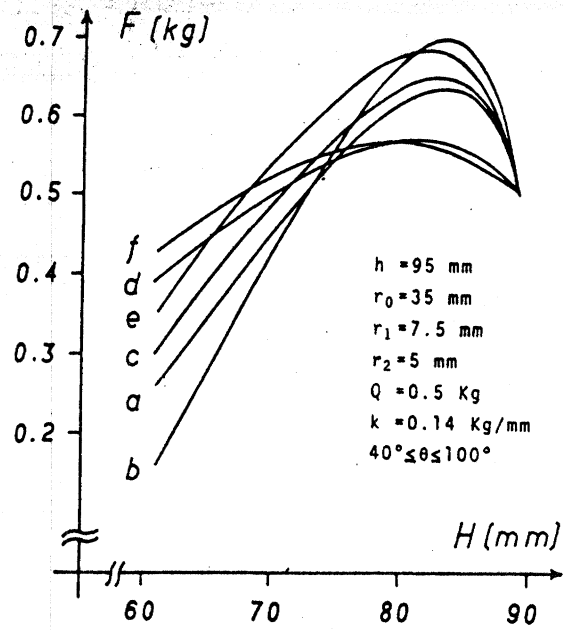


Figure 11: Optimized relation between H and F . The curves (a) and (b) are the results of circular pulleys for the simple and complex mechanisms. The values of b are 18mm and 6.9mm, respectively. The curves (c) and (d) are the results of fuseses of non-circular shape for the simple and complex mechanisms. The values (a,b) are (-0.69, 18.0) and (-0.60, 8.5), respectively. The curves (e) and (f) are the results of flat pulleys of non-circular shape for the simple and complex mechanisms. The values (a,b) are (-0.60, 17.25) and (-0.66, 8.5), respectively.

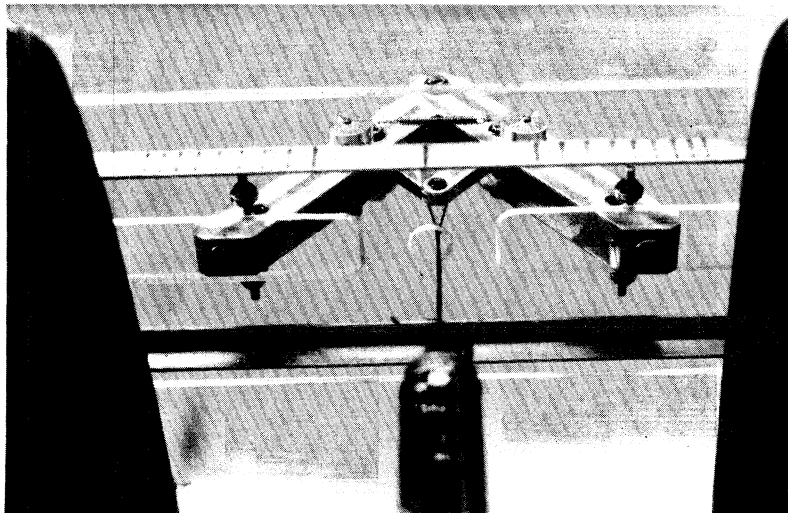


Figure 12: Overview of force measurement by the fabricated mechanism

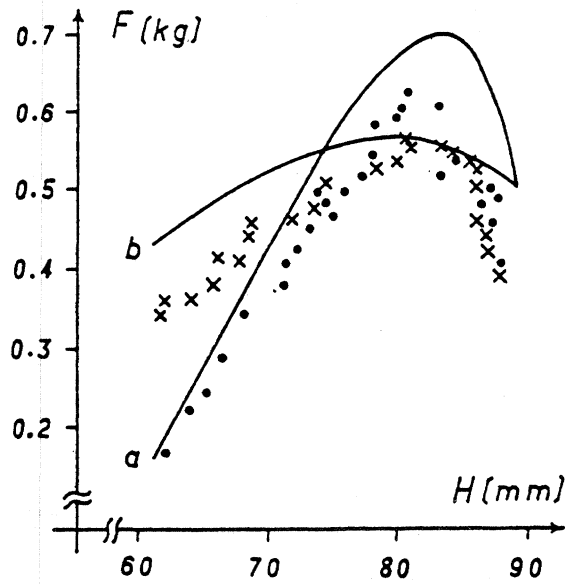


Figure 13: Relationships between F versus H of the complex mechanism. Curves a and b are the calculated results relating to the circular and non-circular pulleys. Dot and cross marks are the experimental results relating to those pulleys, respectively.

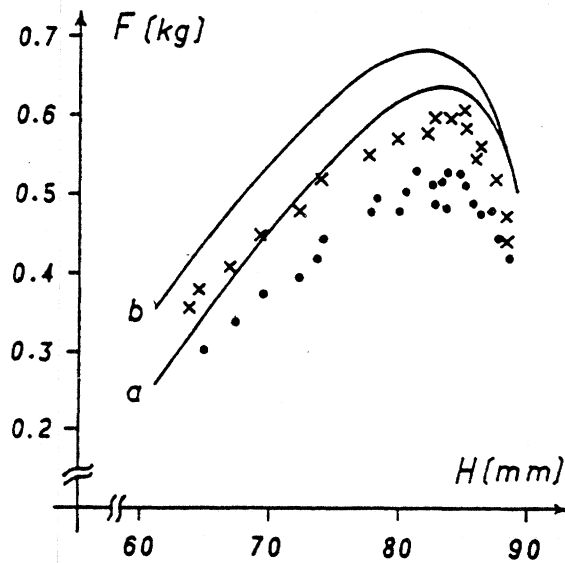


Figure 14: Relationships between F versus H of the simple mechanism. Curves a and b are the calculated results relating to the circular and non-circular pulleys. Dot and cross marks are the experimental results relating to those pulleys, respectively.

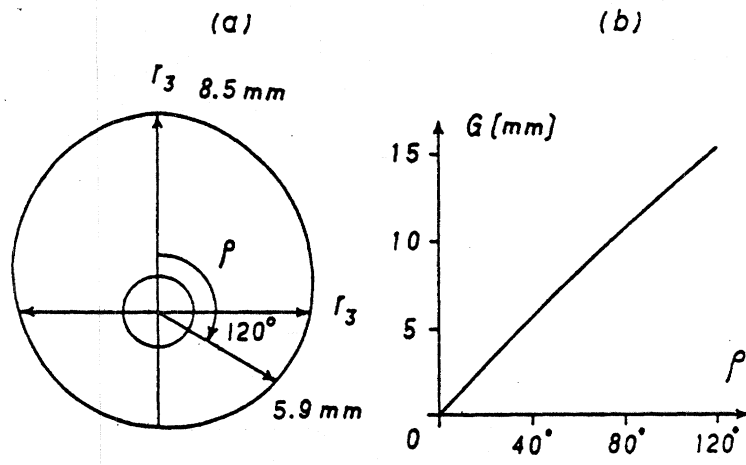


Figure 15: Fabricated pulleys which are used to obtain the curve b in Fig. 13; (a) profile of the groove, (b) characteristics of the ρ versus G .

